

Phenotyping of an *in Vitro* Model of Ischemic Penumbra by iTRAQ-Based Shotgun Quantitative Proteomics

Arnab Datta,[†] Jung Eun Park,[†] Xin Li,[†] Huoming Zhang,[†] Zhi Shan Ho,[†] Klaus Heese,[†]
 Sai Kiang Lim,[‡] James P. Tam,[†] and Siu Kwan Sze^{*†}

School of Biological Sciences, Nanyang Technological University, 60 Nanyang Drive, Singapore 637551, and
 Institute of Medical Biology, A*STAR, 8A Biomedical Grove, Immunos, Singapore 138648

Received September 15, 2009

Cerebral ischemia is a major cause of death and long-term disability worldwide. Ischemic penumbra, the electrically silent but metabolically viable perifocal brain tissue, is the target for the much elusive stroke therapy. To characterize the molecular events of the dynamic penumbra, we applied an iTRAQ-based shotgun proteomic approach in an *in vitro* neuronal model, using the rat B104 neuroblastoma cell line. Various functional and cytometric assays were performed to establish the relevant time-point and conditions for ischemia to recapitulate the pathology of the penumbra. Two replicate iTRAQ experiments identified 1796 and 1566 proteins, respectively ($\leq 1.0\%$ false discovery rate). Mining of proteomic data indicated the up-regulation of proteins involved in ammoniogenesis, antiapoptotic, anti-inflammatory and mitochondrial heat shock response and down-regulation of proteins pertaining to antioxidative defense and protein metabolism. Additionally, many proteins (for instance, park7 and VAP-A) involved in the chronic neurological disorders (such as Alzheimer's disease, Parkinson's disease or Bipolar disorder) were also regulated in this model of acute neuronal injury. Our results also provide preliminary evidence about the presence of a relative glucose paradox under *in vitro* conditions indicating possible application of this cell system to study the mechanisms of transient protection induced by concomitant glucose deprivation under hypoxia. In conclusion, our study shows the potential application of iTRAQ-based quantitative proteomics for the elucidation of pathophysiology and the discovery of novel therapeutic targets in the field of neuroproteomics.

Keywords: ischemic penumbra • B104 cell line • iTRAQ • neuroproteomics • oxygen glucose deprivation • mitochondrial permeability transition

Introduction

Cerebral ischemia, the most common form of acute neurological injury, is the leading cause of mortality and morbidity throughout the world. This results in significant socioeconomic burden due to the lack of effective neuroprotective or restorative therapy.¹

The quest for an effective stroke therapy began with the discovery of ischemic penumbra in the late 1970s.² This electrically silent hypoperfused tissue present between normal and critically compromised brain region was found to be metabolically viable and, hence, theoretically salvageable. Subsequently, extensive physiologic, mechanistic and diagnostic characterization of the penumbra has identified the critical biochemical events (for example, lactic acidosis, glutamate excitotoxicity, calcium overload, free radical stress) that cause eventual metabolic shutdown and cell death in the ischemic penumbra.³

The translation of hypothesis into effective neuroprotective therapies still remains elusive as hundreds of novel compounds targeting a plethora of therapeutic targets have failed at different stages of clinical trials. Notably, most of these experimental therapeutic compounds targeted only one or a few proteins. So, the emphasis is now gradually shifting toward a combination therapy involving multiple targets.¹ However, the traditional reductionist approach is not comprehensive enough to identify and characterize multiple targets relevant to the complex stroke pathophysiology. This apparent methodological void necessitates the use of techniques that can provide a global protein landscape in an appropriate model of cerebral ischemia to better understand the dynamic interactions of multiple targets.

The recent advances in the field of proteomics and bioinformatics have made it possible to profile the comprehensive protein expression levels of the whole tissue, cells and even subcellular organelle in health and disease. More importantly, the proteome from different conditions or cell-lines can now be quantified in a single experiment with various quantitative proteomic techniques. Isobaric tag for relative and absolute quantification (iTRAQ)⁴ is a unique *in vitro* isotopic labeling strategy for simultaneously quantifying 4- or 8-plex samples.

* Corresponding author: Siu Kwan Sze, Ph.D., School of Biological Sciences, Nanyang Technological University, 60 Nanyang Drive, Singapore 637551. Tel: (+65)6514-1006. Fax: (+65)6791-3856. E-mail: sksze@ntu.edu.sg.

[†] Nanyang Technological University.

[‡] Institute of Medical Biology, A*STAR.

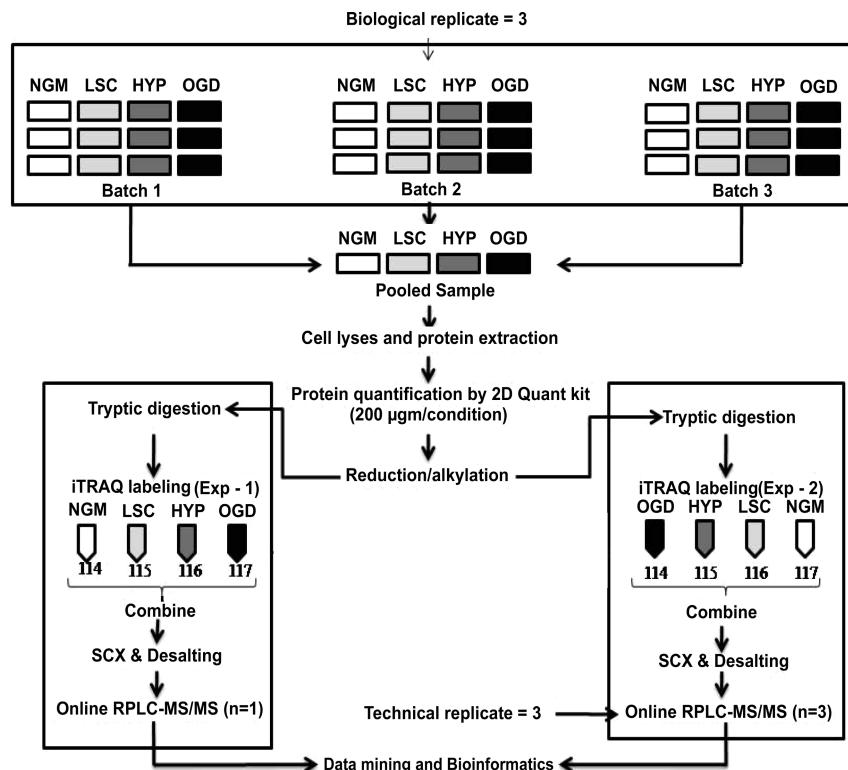


Figure 1. Schematic representation of the experimental design showing biological and technical replicates.

It has a diverse range of application in mammalian and other systems to effectively capture the dynamic proteome in a quantitative manner. Despite its popularity, only a few applications of this high-throughput technique have been documented in the area of neuroproteomics.⁵ Neuroproteomics of tissue suffers from the inherent heterogeneity of the brain, thus, making it difficult to distinguish the origin of a protein coming from the various cell types.⁶ For the same reason, choosing primary cultured cells or using organotypic cultures may not be that relevant for mechanistic studies by a quantitative proteomic approach. This results in a dearth of reliable quantitative data for the study of the pathology of cerebral ischemia. On the other hand, a large number of studies have been documented that looked separately into one or few proteins using *in vitro* models of cerebral hypoxia and ischemia based on primary, organotypic or cell line systems.^{7–9} However, they lack the power of comprehensiveness that is the inherent strength of the quantitative proteomic approach.

To address this research gap, we applied iTRAQ-based shotgun proteomics (iTRAQ-2DLC-MS/MS) on an *in vitro* penumbral model of neuronal hypoxia and ischemia. As neurons are the pivotal but the most vulnerable component of the neurovascular unit in the central nervous system (CNS) during ischemia, a neuronal cell line was chosen for the generation of an appropriate *in vitro* model. The B104 neuroblastoma cell-line, derived from the rat CNS, was used as it displays typical neuronal characteristics (including membrane excitability, expression of neurotransmitters, neuron-specific receptors and the 14-3-2 neuron-specific protein).¹⁰ To establish an *in vitro* penumbral model that simulates the salvageable part of the ischemic brain, various functional and cytometric assays, including MTT cell viability assay, lactate dehydrogenase (LDH) efflux assay, flow cytometric assays for mitochondrial permeability transition (MPT) pore opening and apoptosis,

were performed on glucose-deprived hypoxic cells to establish the correct time-point and conditions to mimic the pathology of penumbra. Afterward, iTRAQ was applied to obtain a quantitative fingerprint of the pathologically relevant proteome to understand the neuroprotective mechanisms. The quantitative proteomic results indicated that the ischemic stress induced two mutually competing protective and deleterious pathways in this penumbral model. Therefore, promoting the protective and suppressing the deleterious pathways in a compatible combination could provide a novel strategy for neuroprotective intervention.

Experimental Procedures

Reagents. Unless indicated, all reagents used for the biochemical methods were purchased from Sigma-Aldrich (Sigma-Aldrich, WI).

Cell Culture. The B104 rat neuroblastoma cell line (kindly provided by Dr. Kazuhiro Ikenaka; Okazaki National Research Center, Aichi prefecture, Japan) was cultured in Dulbecco's Modified Eagle Medium with high glucose (4500 mg/L) and L-alanyl-L-glutamine (862 mg/L), supplemented with 1% Pen-Strep (Streptomycin (10 000 µg/mL) and Penicillin (10 000 units/mL)), and 10% fetal bovine serum (FBS). Cells were grown as a monolayer at 37 °C in a humidified incubator containing 95% air/5% CO₂. All experiments were performed within 8–16 passages of the cells. All media and supplements were bought from Gibco, Invitrogen (Invitrogen, Carlsbad, CA).

***In Vitro* Hypoxia-Ischemia Model.** Cells were cultured for at least 24 h to achieve a confluency of 50–70% before subjecting to four different conditions (Figure 1), such as:

- i. Normal growth media (NGM): Normal high glucose media, 10% FBS and 1% penstrep
- ii. Low serum control (LSC): Normal high glucose media, 1% FBS and 1% penstrep

- iii. Hypoxia (HYP): Same as LSC, but with oxygen deprivation
- iv. Oxygen-glucose deprivation (OGD): Glucose-pyruvate free media, 1% FBS and 1% penstrep with oxygen deprivation.

To induce HYP and OGD, cells were washed with deoxygenated normal and glucose-free media, respectively, for HYP and OGD condition. They were transferred into a humidified airtight chamber (Modular Incubator Chamber (MIC-101), Billups-Rothenberg, Inc., Del Mar, CA) and flushed with hypoxia gas (95% N₂/5% CO₂). Subsequently, the chamber was kept at 37 °C in the humidified incubator for different durations (2, 4, 6, and 8 h). The control (LSC and NGM) plates were directly put inside the humidified incubator without being exposed to hypoxia.

Preproteomic Model Validation. The cytometric and plate-based assays were repeated with three independent biological samples; Three experimental replicates were performed for each sample.

1. 3-(4,5-Dimethylthiazol-2-yl)-2,5-diphenyltetrazolium Bromide (MTT) Assay. The metabolic activity of the cells (cell viability) was assessed using MTT/formazan-assay.¹¹ Cells in serum-free media were incubated for 2 h with MTT (0.5 mg/mL) at 37 °C, 5% CO₂, to allow the yellow MTT to be metabolized to purple formazan. It was then dissolved in DMSO and the optical density was measured at 570 nm using a monochromator microplate reader (Safire², Tecan Group Ltd., Männedorf, Switzerland). The optical density was normalized with the number of cells (determined by trypan blue staining in a hemocytometer) for each sample after subtracting the background obtained using a cell-free control. Viability of the cells in NGM was set as 100% to calculate the relative metabolic activity as a percentage of control.

2. LDH Efflux Assay. LDH activity of the culture medium was assessed¹² colorimetrically using the Cytotoxicity Detection Kit^{PLUS} (Roche, Mannheim, Germany) following the manufacturer's method. Cell death was measured with respect to the LSC sample which was set at 100% after subtracting the background that consisted of normal or glucose-free media.

3. Flow Cytometric Assessment of MPT Pore Opening. This experiment was performed with the MitoProbe Transition Pore Assay kit (Invitrogen, Eugene, OR) following the manufacturer's protocol.¹³ In brief, prewarmed PBS-washed cells were resuspended in Hanks' Balance Salt Solution with calcium (HBSS/Ca) (10⁶ cells/mL). Three aliquots (10⁶ cells/sample) were incubated with calcein AM (2 μM), calcein AM + cobalt chloride (CoCl₂) (80 mM), and calcein AM + CoCl₂ + ionomycin (0.1 mM), respectively, at 37 °C for 15 min in dark. The first and third one acted as control, whereas the change in the fluorescence intensity for the second tube (calcein AM + CoCl₂) between different conditions indicated the continuous activation of MPT pores. Data acquisition (10⁴ events/sample) was performed using the CellQuestPro software in BD FACSCalibur flow cytometer (Becton Dickinson, San Jose, CA).

4. Apoptosis Measurement by Flow Cytometry. This experiment was performed using the commercial BD Pharmingen FITC Annexin V Apoptosis Detection kit I (BD Biosciences, San Diego, CA). Briefly, the trypsin-detached and washed cells from each condition were resuspended in binding buffer (10 mM HEPES/NaOH (pH 7.4), 140 mM NaCl, 2.5 mM CaCl₂) (10⁶ cells/mL).¹⁴ Aliquots of 10⁵ cells were stained simultaneously with 5 μL of Annexin V-FITC and propidium iodide (PI) (50 μg/mL) for 15 min at room temperature in dark. The percentage of intermediate or late stage of apoptosis was determined from

the number of Annexin V(+)/PI(+) cells using the CellQuest Pro software.

Proteomics. 1. Experimental Design. The hypoxia-ischemia experiment was performed three times using three different passages of the cell line ranging between passage-9 and 12. On each occasion, there were at least three experimental replicates for each condition (namely, NGM, LSC, HYP, and OGD). Finally, cells for the same condition obtained from separate experiments were pooled in order to collate sufficient quantity of cells and at the same time to normalize biological variations. Two iTRAQ experiments were conducted from the same pooled cell lysate using an antiparallel labeling strategy (Figure 1). This was adopted purposefully to minimize variations due to the potential nonuniform labeling efficiency for the same target peptide among different labels. Technical replicate with respect to mass spectrometry was set at three (Experiment 2, see Figure 1) as multiple injections give better coverage of the target proteome with superior statistical consistency. This is especially true for single peptide proteins as more MS/MS spectral evidence was obtained from multiple injections leading to a higher confidence of peptide identification and quantification.¹⁵ The design is depicted in the Figure 1.

2. Sample Preparation. The harvested cells were lysed at 4 °C with an ice-cold lysis buffer (0.5% SDS, 0.5 M triethylammonium bicarbonate, Complete Protease Inhibitor Cocktail (Roche) and phosphatase inhibitor cocktail (PhosSTOP, Roche)) with intermittent vortexing and sonication using a Vibra Cell ultrasonic processor (Jencon, Leighton Buzzard, Bedfordshire, U.K.). The lysate was centrifuged at 20 000g for 45 min at 4 °C and supernatant was stored at -20 °C. Protein quantification was performed using 2-D Quant kit (Amersham Biosciences, Piscataway, NJ). Accordingly, 200 μg of protein was taken from each condition for the subsequent iTRAQ experiments.

3. iTRAQ Labeling. iTRAQ labeling was carried out using commercial reagents (iTRAQ Reagent Multi-Plex kit, Applied Biosystem, Foster City, CA) based on the manufacturer's protocol with minor modifications. Briefly, the cell lysates were reduced, alkylated and diluted 10 times before digesting overnight with sequencing grade modified trypsin (Promega, Madison, WI) with a mass ratio of 1:50 (trypsin/protein) at 37 °C. The dried peptides were then labeled (Figure 1) with respective isobaric tags, incubated at room temperature for 2 h before being combined and vacuum centrifuged to dryness.

4. Strong Cation Exchange (SCX) Chromatography. A total of 800 μg of iTRAQ-labeled peptide was reconstituted into 200 μL of Buffer A (10 mM KH₂PO₄, 25% acetonitrile (ACN), pH 2.85) and fractionated using a 200 × 4.6 mm, 5 μm particle size; 200 Å pore size PolySULFOETHYL A SCX column (PolyLC, Columbia, MD) on a Shimadzu HPLC system (Kyoto, Japan) at a flow rate of 1 mL/min. Buffer B consisted of 10 mM KH₂PO₄, 25% ACN, 500 mM KCl at pH 3.0. The 50 min HPLC gradient was composed of 100% buffer A for 5 min; 0–20% buffer B for 15 min; then 20–40% buffer B for 10 min; followed by 40–100% buffer B for 5 min, and finally 100% buffer A for 10 min. The chromatogram was recorded at 218 nm. A total of 21 fractions were collected after pooling, dried in a vacuum centrifuge and desalted with Sep-Pak Vac C18 cartridges (Waters, Milford, MA). The desalted and dried sample was reconstituted with 0.1% FA for LC-MS/MS analysis.

5. LC-MS/MS Analysis Using Q-STAR. Each sample was analyzed three times using a Q-Star Elite mass spectrometer (Applied Biosystems/MDS SCIEX), coupled with an online

Table 1. Summary of the Preproteomic Model Validation Using Functional and Cytometric Assays

time-point	% LDH cytotoxicity (mean ± SEM)		% MTT viability (mean ± SEM)		intermediate/end stage of apoptosis or necrosis (Annexin V ⁺ /PI ⁺)		MPT pore status	
	HYP	OGD	HYP	OGD	HYP	OGD	HYP	OGD
4 h	111.4 ± 10.5	114.5 ± 2.1	83.2 ± 1.9	82.0 ± 3.5	5.0 ± 0.4	3.3 ± 0.1	closed	closed
6 h	105.1 ± 3.7	139.9 ± 8.7	66.2 ± 2.1	66.5 ± 2.2	NA	NA	closed	closed
8 h	97.8 ± 1.6	147.0 ± 6.7	77.7 ± 3.3	72.0 ± 1.2	NA	NA	closed	p/o ^a

^a P/o: partially open.

Shimadzu microflow HPLC system. For each analysis, 30 μ L of peptide mixture was injected and separated on a home-packed nanobored C18 column with a picofrit nanospray tip (75 μ m i.d. \times 15 cm, 5 μ m particles) (New Objectives, Wubrun, MA). The separation was performed at a constant flow rate of 30 μ L/min with a splitter to get an effective flow rate of 0.2 μ L/min. The mass spectrometer was set to perform data acquisition in the positive ion mode, with a selected mass range of 300–2000 *m/z*. Peptides with +2 to +4 charge states were selected for MS/MS. The three most abundant peptides above 5 count threshold were selected for MS/MS and each selected target ion was dynamically excluded for 30 s with \pm 30 mDa mass tolerance. Smart information-dependent acquisition (IDA) was activated with automatic collision energy and automatic MS/MS accumulation. The fragment intensity multiplier was set to 20 and maximum accumulation time was 2 s. The peak areas of the iTRAQ reporter ions reflect the relative abundance of the proteins in the samples.

6. Mass Spectrometric Raw Data Analysis. The data acquisition was performed using the Analyst QS 2.0 software (Applied Biosystems/MDS SCIEX). Protein identification and quantification were performed using ProteinPilot Software 2.0.1, Revision Number: 67476 (Applied Biosystems, Foster City, CA). The Paragon algorithm in the ProteinPilot software was used for the peptide identification which was further processed by Pro Group algorithm where isoform-specific quantification was adopted to trace the differences between expressions of various isoforms. User defined parameters were as follows: (i) Sample Type, iTRAQ 4-plex (Peptide Labeled); (ii) Cysteine alkylation, MMTS; (iii) Digestion, Trypsin; (iv) Instrument, QSTAR Elite ESI; (v) Special factors, None; (vi) Species, None; (vii) Specify Processing, Quantitate; (viii) ID Focus, biological modifications, amino acid substitutions; (ix) Database, concatenated 'target' (IPI rat; version 3.40; 40 389 sequences and 20 549 266 residues) and 'decoy' (the corresponding reverse sequences); (x) Search effort, thorough. For iTRAQ quantitation, the peptide for quantification was automatically selected by Pro Group algorithm to calculate the reporter peak area, error factor (EF) and *p*-value. The resulting data set was auto bias-corrected to get rid of any variations imparted due to the unequal mixing during combining different labeled samples.

Postproteomic Data Verification with RT-PCR. Total RNA was isolated using TRIzol reagent (Invitrogen) according to the manufacturer's protocol and quantified with NanoDrop ND-1000 (NanoDrop Technologies, Wilmington, DE) to measure the concentration in micrograms per microliter (μ g/ μ L). Specific primers were designed by using open-source primer 3.0 software for Elongation factor 2 (EF-2), annexin I, glutamate dehydrogenase (GDH) (Supplementary Table 1). α -Actinin was used as internal control to check the efficiency of cDNA synthesis and PCR amplification. Two micrograms of RNA was used for cDNA synthesis and amplified using primers for EF-

2, annexin I, GDH and α -Actinin. PCR products were separated by 1.5% agarose gel electrophoresis.

Statistical Analysis. Experimental data were presented as the mean of each condition \pm SEM. The *n* value indicates the number of replicate readings from same or different experiments. One-way ANOVA followed by post hoc Dunnett's multiple comparison test was performed for comparing HYP or OGD condition with NGM or LSC depending on the experiment. Statistical significance was accepted at **p* < 0.05, ***p* < 0.01.

Results and Discussion

The affected brain tissue in cerebral ischemia suffers from partial deprivation of oxygen, glucose and serum. There exist a gradient of injury radiating out from the epicenter of the affected area (called core of injury) to the adjacent tissue in decreasing insult severity. The penumbra represents the intermediate electrically silent but metabolically viable tissue and is in a transitional phase where competing protective and deleterious pathways remain in a dynamic equilibrium until the later predominates to seal the fate of the affected cell. Therefore, penumbra is theoretically salvageable, if the equilibrium could be shifted by stimulating the protective pathways. Here we aim to elucidate the proteomic changes in stroke pathophysiology as a means to discover therapeutic targets for clinical neuroprotective or neurorestorative therapy.

The *in vitro* OGD or HYP were induced in partially serum-deprived media containing 1% serum (10% normal supply) to mimic the partial depletion of blood supply. NGM (high glucose with 10% serum) that simulates healthy brain tissue with normal supply of serum and nutrients served as the central control. LSC (high glucose with 1% serum) was included to detect protein expression changes due to serum deprivation only. As most of the reported *in vitro* ischemia experiments were performed in a time scale between 0.5 and 10 h,^{7–9} we employed mutually complementary functional and cytometric assays to determine the optimal time-point for unraveling the endogenous protective mechanisms. This not only served to validate the model by avoiding batch variations between replicate biological experiments (due to difference in cell age, culture or experimental conditions), but also helped in selecting the most relevant time-point to recapitulate the penumbral condition for proteomic experiment.

MTT and LDH Assay. Time dependent MTT assay (Table 1 and Figure 2) was performed to measure the metabolic activity (mitochondrial dehydrogenase activity)¹⁶ of the cells following *in vitro* hypoxic or ischemic stress. MTT assay indicated significant decrease in metabolic activity after 4, 6, and 8 h of hypoxic and OGD stress. We then assessed the LDH activity of the culture supernatant after 4, 6, and 8 h of induced stress as an indicator of the overall cytotoxicity and relative membrane

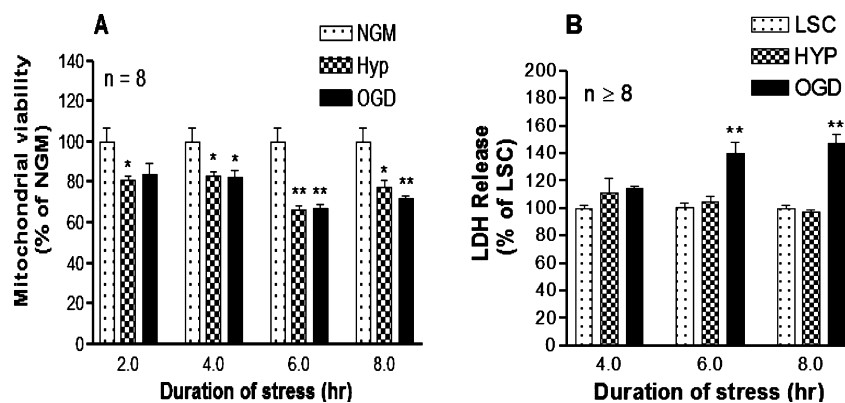


Figure 2. Temporal characterization (2–8 h) of *in vitro* HYP and OGD (ischemia) using functional assays. (A) MTT Assay: Time-dependent changes (2, 4, 6, 8 h) in the mitochondrial redox potential, indicating a significant decrease in metabolic activity at time points post 4 h. (B) LDH Assay: cell death as measured by LDH efflux into the surrounding medium. Note the gradual increase in cell death following 4, 6, and 8 h of OGD. Data represented as mean \pm SEM ($n \geq 8$), calculated from at least 3 experimental runs where * $p < 0.05$, ** $p < 0.01$ vs NGM or LSC using one-way ANOVA test.

integrity of the neuronal cells. As shown in Table 1 and Figure 2, LDH release progressively increased in OGD to reach $\sim 147\%$ post 8 h of stress, while LSC and HYP did not show significant increase in membrane permeability for LDH up to 8 h.

Flow Cytometric Detection of MPT Pore Activation and Apoptosis. To further confirm the presence of significant cellular damage after 6 h of OGD stress as indicated above, cytometric assays to assess mitochondrial function and cellular apoptosis were performed.

Opening of MPT pore indicates a transition from reversible to irreversible cellular damage that induces cell death by apoptosis and necrosis after ischemia/reperfusion injury.^{17,18} Mitochondrial function was assessed with the MitoProbe Transition Pore Assay Kit to characterize the temporal profile of mitochondrial permeability transition pore opening induced by the dissipation of the electrochemical proton gradient after HYP and OGD. As seen in Figure 3A–C, OGD caused a gradual increase in MPT pore opening starting at 6 h and continued until 8 h. In contrast, HYP did not elicit a MPT response as indicated by the lack of changes in the calcein fluorescence (Figure 3D). These observations which were consistent with the results of the LDH assay suggest that OGD become more cytotoxic than HYP with increasing duration of stress.

As irreversible mitochondrial damage measured by MPT assay began at 6 h of OGD stress, 4 h of OGD may induce a stressed but salvageable cellular state that is equivalent to the penumbral condition in cerebral ischemia. To evaluate this hypothesis, the extent of apoptosis at 4 h post OGD was assayed using Annexin V-FITC Apoptosis Detection Kit. Consistent with the observations of LDH and MPT pore assay, neither HYP nor OGD induced significant apoptosis ($<5.0\%$) after 4 h of exposure to stress (Table 1, Supplementary Figure 1). On the basis of the above results (Table 1), 4 h was selected as the most suitable time-point for hypoxia-ischemia experiment to mimic the penumbra for our proteomic profiling as the ischemic cells did not show significant membrane damage ($<15\%$ increase in LDH release), MPT pore formation or apoptosis.

iTRAQ Results. To understand the global proteomic changes that occur in the penumbral state, protein extracts from the control cells (NGM and LSC) and cells exposed to 4 h of OGD or HYP were processed as described in the Experimental Procedures. Totally, four MS runs were compared from two replicate iTRAQ experiments (iTRAQ-1, 1 MS run and iTRAQ-

2, 3 MS runs, see Figure 1). The three technical replicates were combined during database searching to obtain the iTRAQ-2 data set. This was formally analyzed, whereas the iTRAQ-1 data set was kept as a reference to measure the experimental variation.

The quality of the sample preparation was determined by plotting the distribution of the proteins according to their theoretical molecular weight (MW) and theoretical pI values as depicted in Supplementary Figure 2. The presence of proteins covering a wide MW spectrum from high (>200 kDa) to low (<15 kDa) and also a wide pI range from acidic ($pI < 4$) to basic ($pI > 11$) character indicated an extensive representation of the whole proteome in our data set.

To minimize the false positive identification of proteins, a strict cutoff of unused ProtScore ≥ 2 was used as the qualification criteria, which corresponds to a peptide confidence level of 99%. With this filter, the corresponding false discovery rate (FDR) was calculated from the decoy hits. iTRAQ-1 and iTRAQ-2 were able to identify 1566 and 1796 proteins, respectively, with a FDR of $\leq 1.0\%$. Forty percent of the proteins have more than 5 peptides in iTRAQ-2 data set, whereas only around 6% comprised a single peptide having confidence level of 95% (Supplementary Table 2).

A total of 1081 proteins were found to be common in both iTRAQ experiments. Among them, 210 and 139 proteins for HYP and OGD condition, respectively, had significant p -value (<0.05).¹⁹ The p -value assigned by the ProteinPilot software measures the confidence of the real change in protein expression level. The corresponding ratios of these high confidence proteins were plotted to calculate the experimental variation (R^2), which was found to be 0.88 and 0.84, respectively, for HYP and OGD (Figure 4A). It should be mentioned here that OGD corresponds to 117/114 and 114/117, whereas HYP corresponds to 116/114 and 115/117 in iTRAQ-1 and iTRAQ-2 experiment, respectively (Figure 1), thus, involving all iTRAQ labels into consideration.

Subsequently, the meaningful cutoff for the up- or down-regulation was finalized by using the experimental replicate method.^{20,21} The average variation between two iTRAQ experiments were $\pm 8\%$. The experimental variation was less than $\pm 20\%$ for 92% and 97% of the commonly identified proteins with significant ratios ($p < 0.05$) for HYP and OGD stress. In fact, 68% and 79% of the commonly identified proteins had less than

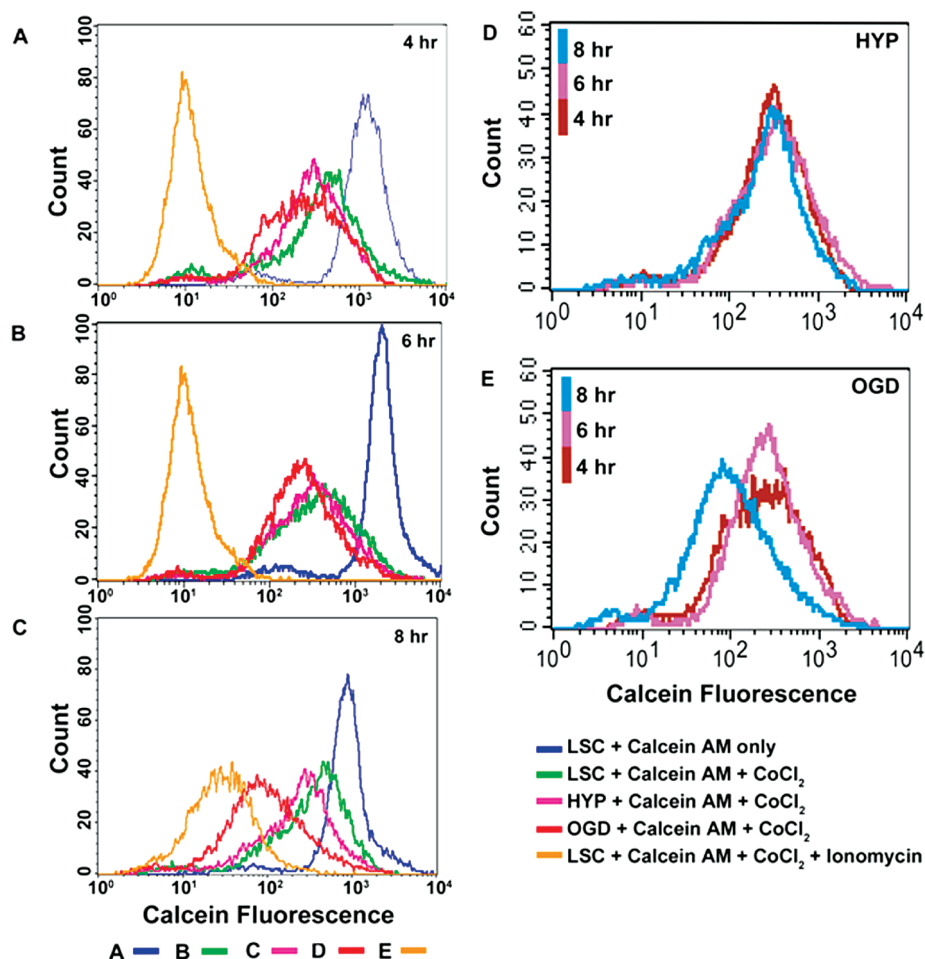


Figure 3. Temporal analysis of MPT pore opening with the MitoProbe Transition Pore Assay Kit using flow cytometry. CoCl_2 specifically quenches the fluorescence of cytosolic calcein. The decrease in calcein fluorescence (x-axis) indicates opening of the MPT pore. The ionophore ionomycin was included as a positive control to trigger MPT pore opening and subsequent loss of mitochondrial calcein fluorescence in the presence of CoCl_2 . (A–C) Gradual opening of the MPT pore following OGD with increasing duration of induced stress. (D and E) An overlay of HYP and OGD at different time points.

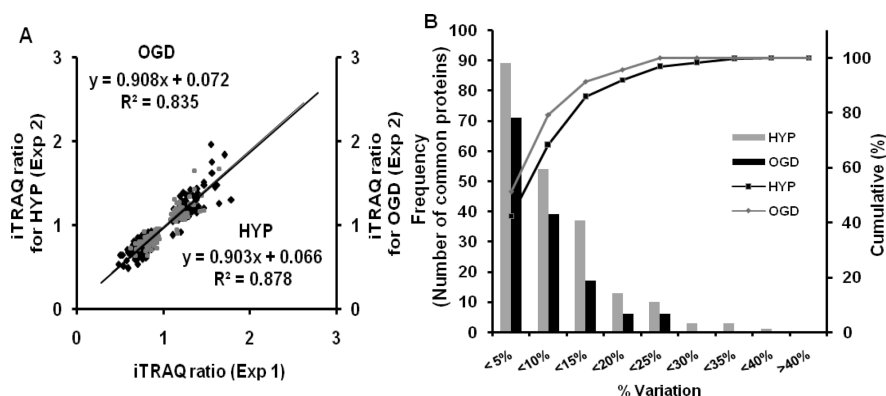


Figure 4. Correlation between two iTRAQ experiments (iTRAQ-1 and iTRAQ-2) and determination of experimental variation using 210 and 139 common proteins (p -value < 0.05) found in both data sets for HYP and OGD, respectively. (A) Plotting of the ratios for OGD and HYP from iTRAQ-1 and iTRAQ-2 data set. The correlation coefficient, R^2 , was 0.88 and 0.84 and the slope was 0.90 for both HYP and OGD, respectively. (B) Percent variation in ratios between the same protein found in both data sets. The primary vertical axis represents the corresponding number of the proteins (bars) having different % variation that was plotted in the horizontal axis. The secondary vertical axis represents the cumulative % of the counted proteins (lines) where 100% equals to 210 and 139 proteins for HYP and OGD, respectively. More than 90% of the proteins had less than 20% of variation justifying the regulation cutoff of 1.2-fold.

$\pm 10\%$ of experimental variation indicating the reliability of our data (Figure 4 B). Based on this, the regulation cutoff was set at 1.2 fold; ratio > 1.20 or < 0.83 was considered as up- or down-regulated.

Verification by RT-PCR. Some of the differentially expressed proteins were verified by RT-PCR. Three proteins representing distinct functional groups in the data set were chosen. The EF-2 had shown down-regulation, whereas annexin I and GDH were

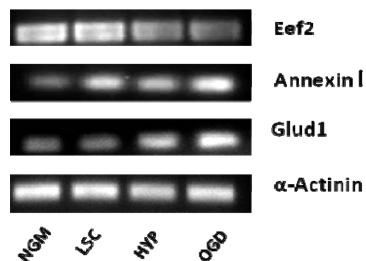


Figure 5. Validation of iTRAQ results on selected proteins using RT-PCR. EF-2 was down-regulated, and annexin1 and GDH were up-regulated that were consistent with the iTRAQ results. α -Actinin that did not show any change in the iTRAQ data set was used as a control. mRNA was collected from the same batch of cells that were used for the iTRAQ experiments.

up-regulated at the mRNA level in HYP and OGD (Figure 5) which were in conformity with the results obtained from iTRAQ.

Unraveling the Ischemic Pathophysiology by analysis of iTRAQ Data Set. The significantly regulated proteins from iTRAQ-2 experiment were functionally analyzed and classified (Table 2) to interpret the molecular events relevant to the pathophysiology of cerebral ischemia.

Proteins Related to Chaperonic Response and Protein Metabolism. Chaperonic proteins showed a mixed response depending on their subcellular locations (Table 2, Figure 6A). There were a general decline in the expression of translation initiation (eIF-5A-1, eIF-4E) and chain elongation (EF-2) proteins during HYP and OGD stress (Table 2, Figure 6B).

Multiparametric imaging in animal models has revealed that protein synthesis in the penumbra was inhibited to conserve ATP supply for the basal metabolic activities.²² Our results were consistent with the metabolic penumbral model as indicated by the down-regulation of the initiation and elongation factors (eIF-4E, eIF-5A-1 and EF-2) (Figure 6B) without a critical decrease in metabolic activity (as seen in MTT assay in Figure 2A) after 4 h of HYP and OGD.

On the other hand, parallel down-regulation of the energy-intensive translation with the coactivation of stress protein expression is indicative of a global stress response. Thus, increasing the chaperonic activity makes the cells better equipped to maintain the critical proteins in optimally folded state under stress while the supply of the newly synthesized proteins is restricted to reduce the workload for the chaperones.²³ This protective mechanism was reflected in our result, as down-regulation of many cytosolic HSPs (CRHSP24, HSP90 alpha, HSP90 beta) along with initiation and elongation factors was accompanied with an upward trend for mitochondria and ER-based chaperones (mtHSP70, HSP75, GRP78) (Figure 6A,B). Mortalin (mtHSP70/Grp75), the heat uninducible mitochondrial chaperone, has been reported to be up-regulated following focal brain ischemia in response to oxidative injury and glucose deprivation.²⁴ GRP78 acts as quality control chaperone for ER and is central to the unfolded protein response in ER.²⁵

Proteins Related to Oxidative Defense. Free radical stress (oxidative and nitrosative) was one of the major factors causing cell death after ischemia of brain and other organs like heart or kidney.^{26,27} Down-regulation of most of the antioxidative proteins (TRX, PRDX6, GSTO1, aldolase reductase-like protein) (Table 2, Figure 6C) positively correlates with the severity of the induced stress in this acute model. TRX is a small (13 kDa), multifunctional protein with a redox-active site having anti-

oxidant, antiapoptotic and neurotrophic activity.²⁸ The immunoreactivity of this isozyme had been diminished in the injured region of the cortex and striatum in a neonatal rat model of hypoxia-ischemia after 4–16 h of injury²⁹ and in the rat middle cerebral artery occlusion model.²⁸ Similarly, PRDX6 has protective effect on the retinal ganglion cells from glutamate and TNF- α induced cytotoxicity by reducing ROS level and NF-kappa- β activation and subsequent Ca²⁺ overload.³⁰

This down-regulation of antioxidant enzymes renders the cells susceptible to the massive burst of free radicals generated during reperfusion, thus, making ischemia-reperfusion a deadly combination with poor outcome in clinical situation. Hence, this result also supports the concept of neuro-protection by ischemic postconditioning either through controlled reperfusion or noninjurious cycles of ischemia-reperfusion.³¹ This will allow the cells sufficient time to revive their antioxidant machinery.

Inflammation and Apoptosis Related Proteins. Annexins belong to the superfamily of calcium and phospholipid-binding proteins having diverse biological functions that include signal transduction to inflammation. Three members of this family, annexin I, II and V, were localized in neurons and glial cells and have potent anti-inflammatory effects through inhibition of PLA₂ activity.³² Several reports have indicated the increased expression of annexins in various pathological conditions like hypoxic-ischemic injury³³ and spinal cord injury.³⁴ Annexin I, II and V were quantified in our model, where the first two (annexin I and II) showed the expected upward trend, consistent with the previous studies (Table 2, Figure 6D).

Prohibitin is present in the mitochondrial inner membrane and plays a chaperonic role in the stabilization of newly synthesized subunits of mitochondrial respiratory enzymes.³⁵ Overexpression of this protein in cardiomyocytes suppressed H₂O₂-induced mitochondria-mediated apoptotic pathways by inhibiting the release of cytochrome c into the cytosol and the opening of the MPT pore.³⁶ Our *in vitro* penumbral model showed an up-regulation of prohibitin-2 (51% in HYP, 25% in OGD; $p = 0.00$) and prohibitin (Table 2, Figure 6D), which may be indicative of an endogenous adaptive response. This finding provides the first illustration of the involvement of this class of chaperone in the pathology of cerebral ischemia to the best of our knowledge.

CLIC4 is a histamine H3 receptor interacting single pass membrane protein which was down-regulated by 29% and 23% (although $p > 0.05$) (Table 2, Figure 6D) in HYP and OGD, respectively. Overexpression of this protein induces apoptosis in several human and mouse cell lines that may be mediated through TNF- α or p53.³⁷ We attribute this yet as another survival strategy for the cells, where the simultaneous up-regulation of the anti-inflammatory (annexin I, II) and anti-apoptotic response (prohibitin, prohibitin2, Bcl-2 like 2) was complemented by the down-regulation of a proapoptotic protein (i.e., CLIC4).

Degradation of Key Proteins. The creatine kinase (CK) catalyzes the reversible interconversion of creatine into phosphocreatine and is a central controller of the cellular energy homeostasis. Particularly, it plays an important role in tissues with large and fluctuating energy demands like the brain and the muscle. All CK isoenzymes are extremely susceptible to enzymatic inactivation by reactive oxygen and nitrogen species generated under ischemic stress.³⁸ Therefore, a significant down-regulation of the cytosolic isozyme creatine kinase type

Table 2. Functional Classification of Regulated Proteins^a

unused prot score	%cov (95)	gene symbol	protein name	LSC/NGM	HYP/NGM	OGD/NGM	subcellular location ^b
Chaperonic Response							
41.4	33.0	Hspa4	Heat shock 70 kDa protein 4	0.92	0.79	0.86	Cytosol
102.8	56.9	Hsp90ca	Heat shock protein HSP 90-alpha	1.00	0.74	0.83	Cytosol
102.8	56.9	Hspcb	Heat shock protein HSP 90-beta	1.04	0.77	0.87	Cytosol
6.1	34.7	Carhsp1	Calcium-regulated heat stable protein 1 (CRHSP24)	0.81	0.6	0.78	Cytosol
9.0	15.7	Hspbp1	Hsp70-binding protein 1 (HspBP1)	0.89	0.7	0.77	Ubiquitous
26.8	30.0	Trap1	Heat shock protein 75 kDa, mitochondrial precursor (HSP75)	1.14	1.29	1.20	Mitochondria
47.6	39.3	Hspa9a	Hspa9a_predicted Stress-70 protein, mitochondrial precursor (GRP75/mtHSP70)	1.05	1.22	1.13	Mitochondria
74.5	48.5	Hspa5	78 kDa glucose-regulated protein precursor (GRP78)	1.07	1.24	1.14	ER lumen
Protein Metabolism							
86.1	39.0	Eef2	Elongation factor 2 (EF-2)	0.98	0.71	0.81	Cytosol
16.0	47.4	Eif5a	Eukaryotic translation initiation factor 5A-1 (eIF-5A-1)	0.91	0.68	0.73	Nucleus
7.5	27.7	Eif4e	Eukaryotic translation initiation factor 4E (eIF-4E)	0.94	0.67	0.80	Cytosol
14.2	30.9	Eif3j ^c	LOC691947; Eif3s1_predicted Eukaryotic translation initiation factor 3 subunit J	0.84	0.69	0.72	Cytosol
Oxidative Defense							
8.1	42.9	Txn1	Thioredoxin (TRX)	0.78	0.49	0.64	Cytosol
10.0	35.3	Prdx6	Peroxiredoxin-6 (PRDX6)	0.91	0.63	0.75	Cytosol, lysosome
13.3	24.9	Txn12	Isoform 1 of Glutaredoxin-3	0.88	0.71	0.81	Cytosol
5.8	15.4	Gsto1	Glutathione transferase omega-1 (GSTO1)	0.98	0.67	0.78	Cytosol
6.1	21.0	Park7	Park7 protein	1.08	0.72	0.82	Cytosol, nucleus, mitochondria
8.8	20.3	Tmx2	Thioredoxin domain-containing protein 14 precursor	1.1	1.28	1.18	ER membrane (probable)
12.7	30.06	Akr1b8	Aldose reductase-like protein	0.97	0.77	0.83	Cytosol
Anti-Inflammatory Protein							
35.2	33.0	Anxa1	Anxa1 44 kDa protein, Annexin I	1.06	1.15	1.25	Ubiquitous
12.3	33.4	Anxa2	Isoform Short of Annexin A2, Annexin II	1.13	1.24	1.22	Secreted
25.3	49.2	Anxa5	Annexin A5, Annexin V	0.92	0.84	0.95	NA
Antiapoptotic Protein							
24.6	42.1	Phb2	Prohibitin-2	1.19	1.51	1.25	Mitochondria
19.9	51.1	Phb	Prohibitin	1.09	1.33	1.18	Mitochondria
27.0	33.0	Pabpn1	Bcl2l2;Pabpn1 similar to Polyadenylate-binding protein 2	1.06	1.15	1.25	Mitochondrion membrane
Proapoptotic Protein							
6.0	24.1	Clic4 ^d	Chloride intracellular channel protein 4 (CLIC4)	0.88	0.71	0.77	ER
Proinflammatory Protein							
13.5	15.6	Ptgs1	Cyclooxygenase-1 (COX-1)	1.13	1.46	1.31	Microsome, Peripheral membrane or ER membrane
Energy Homeostasis							
28.0	55.4	Ckb	Creatine kinase B-type	0.91	0.62	0.70	Cytosol
Cytoskeletal Protein							
26.6	26.2	Dpysl3	Isoform 2 of Dihydropyrimidinase-related protein 3 (DPYSL3)	0.97	0.67	0.75	Cytosol

^a The list contains quantitative information of the proteins from the iTRAQ-2 data set. These proteins have met the criteria (i.e., unused prot score >2.0, change in expression levels of at least 1.2-fold for HYP or OGD relative to NGM, *p*-value <0.05 and EF < 1.4 for all ratios) as defined in the Experimental Procedures. ^b Source: <http://www.uniprot.org/uniprot>. ^c Source; <http://www.ncbi.nlm.nih.gov/sites/entrez>. ^d *p*-value >0.05.

B (38% in HYP, 30% in OGD; *p* = 0.00) (Table 2) indicated a compromised oxidative state of the cells.

On the other hand, glutamate excitotoxicity and oxidative stress can act as the upstream contributing factor that leads to Ca²⁺ ion overload during ischemia. The deleterious consequences of the Ca²⁺ overload is well-known with respect to the stroke pathology, where it causes a widespread activation of proteases (including calpain and caspases), phosphatases, endonucleases and phospholipases (PLA₂) leading to uncontrolled degradation of key cytoskeleton proteins like actin, spectrin, myosin as well as DPYSL3 (Figure 7).³⁹

Simultaneous down-regulation of the calpain substrate, DPYSL3 (33% in HYP, 25% in OGD; *p* = 0.00), and up-regulation of COX-1 probably indicates an early sign of Ca²⁺ overload causing the activation of the calpain and PLA₂-COX1 signaling pathways (Figure 7). It has been shown recently that DPYSL3 degradation in rat cortical neuron can be directly mediated by oxidative stress or glutamate excitotoxicity or through the downstream metabolic product of PLA₂-COX1 signaling, prostaglandin E₂ (PGE₂) which augments the toxic effects of glutamate.³⁹ Thus, up-regulation of annexin I, II in our model may be compensatory in nature by interfering with the PGE₂

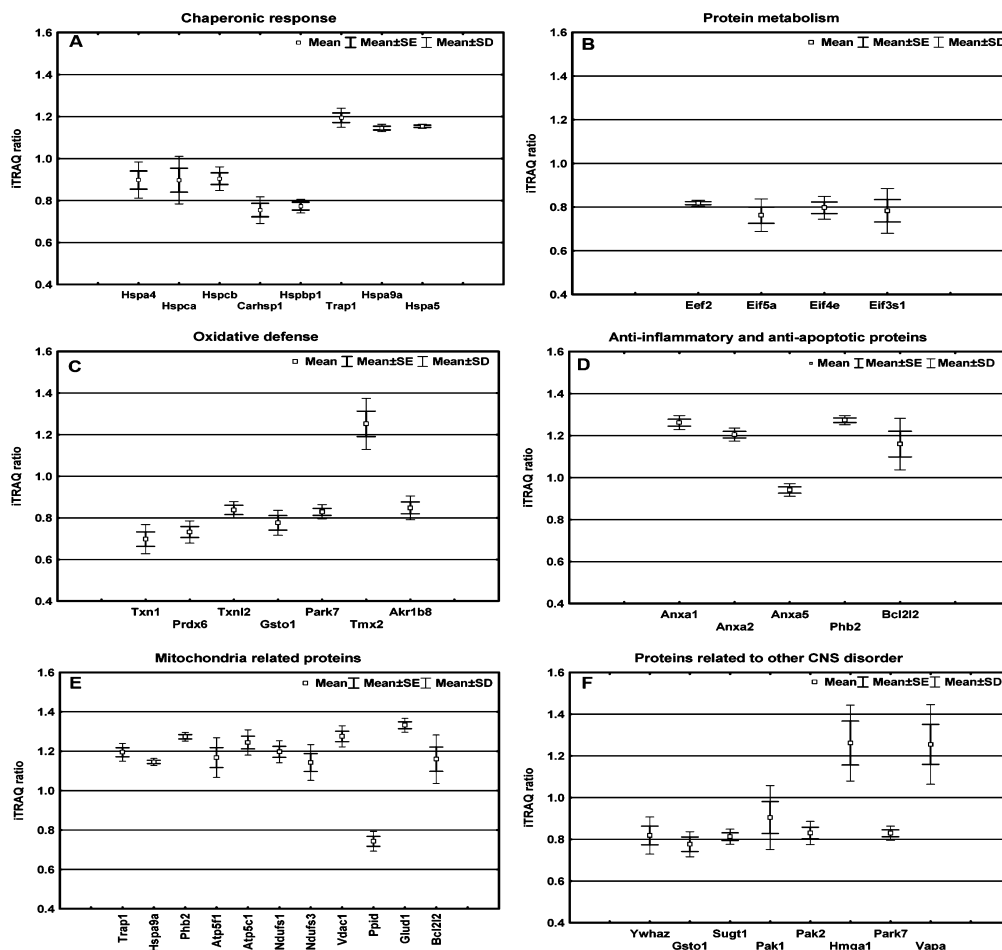


Figure 6. Box whisker plots showing the fingerprint of functionally important proteins after 4 h of OGD stress. Both data sets (iTRAQ-1 and iTRAQ-2) having a total of 4 separate MS runs were combined to get mean, SEM and SD for each ratio. The gene symbols were plotted in the horizontal axis. The vertical axis represents corresponding iTRAQ ratio. (A) The chaperonic cluster showed an upward trend for mitochondrial and ER resident chaperones (Trap1, Hspa9a and Hspa5) unlike cytosolic chaperones which were unaffected or down-regulated. (B) Proteins related to the protein metabolism were down-regulated. (C) Most of the antioxidative enzymes were down-regulated. (D) Anti-inflammatory (anxa1, anxa2) and antiapoptotic (prohibitin, Bcl2l2) proteins were moderately up-regulated. (E) An overview of mitochondrial proteins, where chaperonic response, oxidative phosphorylation (Atp5f1, Atp5c1, Ndufs1, Ndufs3) showed an upward trend unlike proteins involved in the MPT pore (Vdac1, Ppid, Bcl2l2) which showed a mixed trend. The marker for mitochondrial acidosis, Glud1, was significantly up-regulated. (F) Regulated proteins implicated in other neurological disorders.

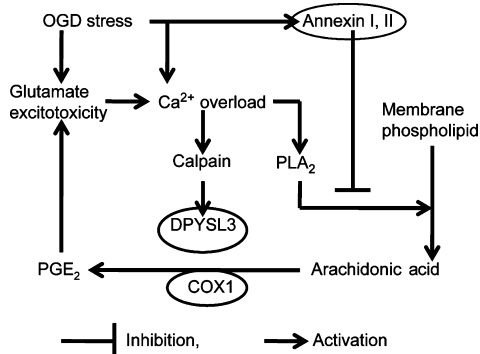


Figure 7. Flowchart of pathways involved in the degradation of DPYSL3. The encircled proteins were significantly regulated in our iTRAQ data set.

generation through the inhibition of PLA₂ and can constitute a novel way of protecting the essential cytoskeletal proteins (Figure 7).

Role of Mitochondria in Ischemic Stress Response. Mitochondria are central to the survival of the neuronal cells

following ischemia by controlling aerobic metabolism and calcium homeostasis. This was revealed by its active participation in the ischemic stress response with many mitochondrial proteins showing significant up-regulation (Table 3, Figure 6E).

Our result indicated metabolic acidosis as seen by the compensatory increase in the expression of GDH (48% in HYP, 34% in OGD; *p* = 0.00) and subsequent catabolism of glutamine.⁴⁰ It was confirmed by the increased expression of GDH at the transcriptional level (Figure 5). Activation of proteins involved in the respiratory chain and chaperonic functions (Table 3) suggested an early stage of hypoxic-ischemic injury as oxidative phosphorylation will be inhibited if mitochondria are depolarized due to the influx of Ca²⁺ ions through an electrophoretic uniporter. This may reflect the cell's desperation for maintaining the ATP supply to sustain the protein synthesis and cytosolic chaperonic activity, both of which were quite depressed as seen in the previous discussion.

The role of mitochondria has been implicated in the intrinsic pathway of the apoptotic cascade where different apoptogenic molecules (e.g., cytochrome c, AIF, Smac/Diablo, DNaseG) are released into the cytosol following a sudden increase in

Table 3. Functional Classification of Mitochondrial Proteins^a

unused prot score	%cov (95)	gene symbol	protein name	LSC/NGM	HYP/NGM	OGD/NGM
Metabolic Acidosis						
36.7	32.1	Glud1	Glutamate dehydrogenase 1, mitochondrial precursor (GDH)	1.20	1.48	1.34
Chaperonic						
26.8	30.0	Trap1	Heat shock protein 75 kDa, mitochondrial precursor (HSP75)	1.14	1.29	1.20
47.6	39.3	Hspa9a	Hspa9a_predicted Stress-70 protein, mitochondrial precursor (GRP75/ mtHSP70)	1.05	1.22	1.13
24.6	42.1	Phb2	Prohibitin-2	1.19	1.51	1.25
19.9	51.1	Phb	Prohibitin	1.09	1.33	1.18
Respiratory Chain						
9.4	16.8	Atp5f1	ATP synthase subunit b, mitochondrial precursor	1.13	1.38	1.27
5.7	3.6	Atp5c1	ATP synthase gamma chain	1.12	1.26	1.25
31.3	29.7	Ndufs1	NADH-ubiquinone oxidoreductase 75 kDa subunit, mitochondrial precursor	1.01	1.26	1.21
14.7	34.5	Ndufs3	predicted NADH dehydrogenase (ubiquinone) Fe-S protein 3	1.06	1.20	1.17
MPT Pore						
22.0	34.3	Vdac1	Voltage-dependent anion-selective channel protein 1(VDAC1)	1.19	1.45	1.25
22.8	36.8	Ppid	40 kDa peptidyl-prolyl <i>cis-trans</i> isomerize, CypD	0.86	0.63	0.72
Apoptosis Related						
27.0	33.0	Pabpn1 /Bcl2l2	Bcl2l2(Bcl2-like-2), Pabpn1 similar to Polyadenylate-binding protein 2	1.06	1.15	1.25
6.0	24.1	Clic4 ^b	Chloride intracellular channel protein 4(CLIC4)	0.88	0.71	0.77

^a The list contains quantitative information of the significantly regulated mitochondrial proteins from the iTRAQ-2 data set. These proteins have met the criteria (i.e., unused prot score >2.0, change in expression level of at least 1.2-fold for HYP or OGD relative to NGM, *p*-value <0.05 and EF < 1.3 for all ratios) as defined in the Experimental Procedures. ^b *p*-value > 0.05.

mitochondrial outer membrane permeability following the MPT.^{41,42} Formation of the MPT pore takes place in response to the Ca²⁺ overload, oxidative stress and ATP depletion. The MPT pore complex is composed of VDAC at OMM (outer mitochondrial membrane), ANT (Adenine nucleotide translocase) in the IMM (inner mitochondrial membrane) and CypD located in the mitochondrial matrix. It has been speculated that overexpression of VDAC under conditions of acute hypoxia-ischemia will encourage its dynamic oligomerization at the outer mitochondrial membrane, thus, permitting the release of proapoptotic proteins from the intermitochondrial space.⁴³ Antiapoptotic members of the Bcl-2 family of proteins (e.g., Bcl-2, Bcl-w) tend to prevent this MPT pore formation probably by blocking the VDAC homodimerization.⁴⁴ The increase in the expression of VDAC1 (45% in HYP, 25% in OGD; *p* = 0.00) in our model, thus, indicates an ominous signal for the cells that have been duly complemented by the increase in protective Bcl2l2 and prohibitin-2.

Brain mitochondria exert a higher calcium threshold to MPT induction compared to other types (heart or liver) of mitochondria.^{45,46} This relative resistance may be a protective mechanism as neurons cannot be renewed in the passage of life. Intriguingly, CypD expression decreases progressively during brain development indicating an inverse relationship with the MPT threshold for Ca²⁺ ion.⁴⁶ In addition, recent reports suggest involvement of CypD in necrotic cell death that is independent of the Bcl-2 family of proteins. CypD along with other components of MPT are also in contention as a promising therapeutic target for ischemia-reperfusion injury of the brain.^{18,47} Thus, the down-regulation (37% in HYP, 28% in OGD; *p* = 0.00) of this essential component of MPT following acute hypoxia-ischemia may constitute an unique survival strategy for the mitochondria in context of the current penumbral model.

The quantitative proteomic result indicates the delicate balance between mutually competing numerous pro- and anti-survival mechanisms in the ischemic penumbra after 4 h of acute hypoxia and ischemia. This indicates that the cells are actively trying to salvage themselves by up-regulating the antiapoptotic and anti-inflammatory proteins including mitochondrial chaperons and enzymes for ammoniogenesis with a concomitant suppression of the protein synthesis. On the other hand, the collapse of the cellular antioxidant machinery and subsequent inactivation of creatine kinase type B, activation of COX1 and calpain mediated breakdown of the cytoskeleton protein, DPYSL3, indicate the accumulating stress, thus, exposing cell's vulnerability toward prolonged hypoxic-ischemic or ischemic-reperfusion injury (Figure 8). This initial phase is crucial for the cells as the pro-death signals eventually outweighs the survival machinery in the later time points when opening of MPT pore causes cell death via apoptosis or necrosis. Hence, it will be interesting to see how the novel or existing pharmacological approaches behave in this model when used alone or in compatible combinations at different time-points (4 or 8 h).

Proteins Related to Chronic Neurological Disorder. We also discovered a set of novel proteins regulated in this acute penumbral model (Table 4, Figure 6F) that have an important implication in different chronic neurological disorders.

Park-7 (also known as DJ-1), which was moderately down-regulated (28% in HYP, 18% in OGD; *p* = 0.00) in our model, was initially discovered as a protein involved in the pathology of Parkinson's disease (PD). Recent reports have indicated a significant protective role of DJ-1 in both *in vitro* and *in vivo* models of stroke, where a loss of DJ-1 increases the vulnerability to excitotoxicity and ischemia.^{48,49} Similarly, the omega class of glutathione *S*-transferase (glutathione-dependent thiol

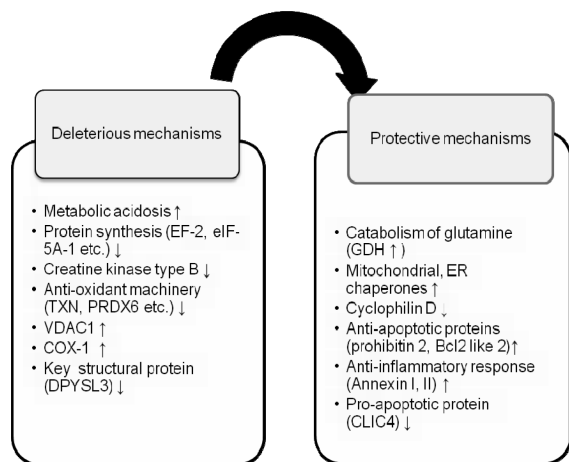


Figure 8. Complex interplay of pro- and antisurvival mechanisms after 4 h of *in vitro* hypoxia and ischemia.

transferase and dehydroascorbate reductase) was another down-regulated multifunctional enzyme in our data set having a protective role against oxidative stress. It has been implicated in a variety of neurological disorders like early onset Alzheimer’s disease (AD), PD, vascular dementia, cerebral atherosclerosis and amyotrophic lateral sclerosis.^{50–52} Thus, our results corroborate previous studies which showed a general decline of the antioxidant machinery in the current model.

The down-regulated 14-3-3 protein zeta/delta is a highly abundant adaptor protein and reported as a hub in the genetic network of AD and aging.⁵³ Another down-regulated candidate, suppressor of G2 allele of SKP1 homologue, has been suggested as a possible marker of degenerating neurons in AD based on its decreased immunostaining in the AD-affected cortex.⁵⁴ Similarly, a recent report relates PAKs (serine/threonine class of protein kinases), that was moderately down-regulated at the level of total protein, to synaptic loss and cognitive deficits in the AD patients.⁵⁵

The moderately up-regulated vesicle-associated membrane protein-associated protein A (VAP-A) (36% in HYP, $p = 0.002$; 28% in OGD, $p = 0.017$) is a single-pass type IV membrane protein that interacts with presynaptic proteins and is necessary for vesicular neurotransmission. Recently, polymorphism of VAP-A has been linked to bipolar disorder (BD).⁵⁶ The other

member of this ‘up-regulation’ group, HMG-I/Y is a nucleus-resident nonhistone protein, overexpression of which has been observed in the brain tissue of sporadic AD patients.⁵⁷

Although the down-regulation of the above proteins can be explained by the correlative decrease in the overall rate of protein synthesis or increased turnover, the significant up-regulation of some of them (HMG-I/Y, VAP-A) (Figure 6F) is a novel finding in context of this acute model, which necessitates further study to adequately understand their roles in the pathology of cerebral ischemia. Nevertheless, the result clearly indicates the complex interaction and presence of common signaling pathways between radically differing neuropathologies.

Possible Presence of Glucose Paradox. Our result provides evidence to support the existence of a relative “glucose paradox”, which is defined by the aggravation of postischemic outcome due to preischemic hyperglycemia. This phenomenon has only been observed in numerous *in vivo* studies, but a convincing explanation is not available yet. Tentatively, it has been attributed to either lactic acidosis or to the involvement of stress hormones and glucocorticoids.⁵⁸ Here, we demonstrate a similar enigma as our result showed that glucose deprivation did not produce a synergistic damaging effect when coupled with oxygen deprivation (OGD) in the initial phase (4 h) of *in vitro* ischemia. This is evident in the trend of the absolute protein expression in the iTRAQ data set (Tables 2–4) as well as in the functional and cytometric assays. The expected trend was observed in the functional assays when the duration of stress was increased to 6 or 8 h (Figures 2B and 3) as OGD becomes more lethal than HYP. This crucial finding, novel with respect to an *in vitro* system, may be related to the type of cell-line, culture conditions or the experimental design. This further indicates the participation of cell-specific mechanisms as systems level properties, like hormonal interference, can be ruled out in an isolated cell system. Nevertheless, this *in vitro* penumbral model with the neuronal B104 cell line can be used for studying the mechanisms involved in the glucose deprivation-induced transient protection against ischemic insult.

Concluding Remarks

By applying a discovery-driven iTRAQ-based quantitative proteomic approach to a validated *in vitro* neuronal hypoxia-ischemia model, we were able to capture the early stages of

Table 4. Proteins Related to Other CNS Disorders^a

unused prot score	%cov (95)	gene symbol	protein name	LSC/NGM	HYP/NGM	OGD/NGM
Alzheimer’s Disease						
26.0	65.7	Ywhaz	14-3-3 protein zeta/delta	0.76	0.63	0.82
5.8	15.4	Gsto1	Glutathione transferase omega-1(GSTO1)	0.98	0.67	0.78
9.5	17.0	Sugt1	Suppressor of G2 allele of SKP1 homologue	0.92	0.68	0.79
6.4	15.4	Pak1	Serine/threonine-protein kinase PAK 1	0.97	0.76	0.79
10.6	15.3	Pak2	Serine/threonine-protein kinase PAK 2	0.95	0.77	0.85
4.3	41.1	Hmgal	Isoform HMG-I of High mobility group protein HMG-I/HMG-Y	1.18	1.34	1.23
Parkinson’s Disease						
6.1	21.0	Park7	Park7	1.08	0.72	0.82
Bipolar Disorder						
3.7	13.3	Vapa	Vesicle-associated membrane protein-associated protein A (VAP-A)	1.17	1.36	1.28

^a The list contains quantitative information of the significantly regulated proteins related to chronic neurological disorders from the iTRAQ-2 data set. These proteins have met the criteria (i.e., unused prot score >2.0, change in expression level of at least 1.2-fold for HYP or OGD relative to NGM, p -value < 0.05 and EF < 1.3 for all ratios) as defined in the Experimental Procedures.

neuronal response to cerebral hypoxic and ischemic stress. This was achieved even when most of the functional assays fail to differentiate hypoxic and ischemic cells from the normal cells in absence of significant morphological or functional abnormalities. The preproteomic assays confirmed the presence of a therapeutic window for the ischemic penumbra that can potentially be rescued by promoting the protective and suppressing the deleterious pathways. The sheer number of detected proteins (634 and 739 proteins for OGD and HYP, respectively) with quantitative information having acceptable levels of confidence (i.e., p -value < 0.05) (Supplementary Table 2) also makes this iTRAQ-based 2D-LC-MS/MS approach the preferred technique to investigate the underlying molecular mechanisms of cerebral ischemia at the systems level. Moreover, these short-listed proteins can act as a starting point for the follow-up experiments to characterize individual proteins, for example, by RNA interference, to identify potential neuro-protective targets for interventional studies.

Our findings also indicate the probable presence of a relative glucose paradox under *in vitro* condition. Furthermore, many proteins involved in chronic neurological disorders (AD, PD and BD) were changed in this acute neuronal injury model, suggesting the involvement of some common pathways between deleterious neuronal diseases. Concluding, our results show that the iTRAQ-based shotgun proteomic approach not only constitutes a novel way of investigating the pathophysiology of complex diseases in validated models, but can also act as a screening tool in discovery-driven translational research.

Acknowledgment. The authors thank Salil Kumar Bose for critical reading of the manuscript and Manavalan Arulmani for the technical support. This work is supported by grants from the Ministry of Education (ARC: T206B3211) and the Agency for Science, Technology and Research (A*STAR, the Biomedical Research Council, BMRC: 08/1/22/19/575) of Singapore.

Supporting Information Available: Supplementary Figure 1, flow cytometric detection of apoptotic population after 4 h of HYP or OGD. Supplementary Figure 2, distribution of identified proteins from iTRAQ-2 data set (unused prot score >3) according to their molecular weight (MW, kDa) and theoretical pI (pI). Supplementary Table 1, primer sequences for RT-PCR. Supplementary Table 2, quantitative proteomic data set from iTRAQ-2 containing 1796 proteins with unused prot score >3 and FDR = 1.0%; 634 and 739 proteins were detected with $p < 0.05$, respectively, for OGD and HYP. This material is available free of charge via the Internet at <http://pubs.acs.org>.

References

- Zaleska, M. M.; Mercado, M. L. T.; Chavez, J.; Feuerstein, G. Z.; Pangalos, M. N.; Wood, A. The development of stroke therapeutics: Promising mechanisms and translational challenges. *Neuropharmacology* **2009**, *56*, 329–341.
- Astrup, J.; Symon, L.; Branston, N. M.; Lassen, N. E. Cortical evoked potential and extracellular K^+ and H^+ at critical levels of brain ischemia. *Stroke* **1977**, *8* (1), 51–57.
- Lo, E. H. A new penumbra: Transitioning from injury into repair after stroke. *Nat. Med.* **2008**, *14* (5), 497–500.
- Gygi, S. P.; Rist, B.; Gerber, S. A.; Turecek, F.; Gelb, M. H.; Aebersold, R. Quantitative analysis of complex protein mixtures using isotope-coded affinity tags. *Nat. Biotechnol.* **1999**, *17* (10), 994–999.
- Martin, B.; Brennehan, R.; Becker, K. G.; Gucuk, M.; Cole, R. N.; Maudsley, S. iTRAQ analysis of complex proteome alterations in 3xTgAD Alzheimer's mice: Understanding the interface between physiology and disease. *PLoS ONE* **2008**, *3* (7), e2750.
- Tweedie-Cullen, R. Y.; Wollscheid, B.; Livingstone-Zatchej, M.; Mansuy, I. M. Neuroproteomics and the detection of regulatory phosphoproteins. *Curr. Proteomics* **2007**, *4* (4), 209–222.
- Miglio, G.; Varsaldi, F.; Francioli, E.; Battaglia, A.; Canonico, P. L.; Lombardi, G. Cabergoline protects SH-SY5Y neuronal cells in an *in vitro* model of ischemia. *Eur. J. Pharmacol.* **2004**, *489* (3), 157–165.
- Bonde, C.; Norberg, J.; Noer, H.; Zimmer, J. Ionotropic glutamate receptors and glutamate transporters are involved in necrotic neuronal cell death induced by oxygen-glucose deprivation of hippocampal slice cultures. *Neuroscience* **2005**, *136* (3), 779–794.
- Lin, C. H.; Cheng, F. C.; Lu, Y. Z.; Chu, L. F.; Wang, C. H.; Hsueh, C. M. Protection of ischemic brain cells is dependent on astrocyte-derived growth factors and their receptors. *Exp. Neurol.* **2006**, *201* (1), 225–233.
- Bottenstein, J. E.; Sato, G. H. Growth of a rat neuroblastoma cell line in serum free supplemented medium. *Proc. Natl. Acad. Sci. U.S.A.* **1979**, *76* (1), 514–517.
- Mosmann, T. Rapid colorimetric assay for cellular growth and survival: Application to proliferation and cytotoxicity assays. *J. Immunol. Methods* **1983**, *65* (1–2), 55–63.
- Legrand, C.; Bour, J. M.; Jacob, C.; Capiamont, J.; Martial, A.; Marc, A.; Wudtke, M.; Kretzmer, G.; Demangel, C.; Duval, D.; Hache, J. Lactate dehydrogenase (LDH) activity of the number of dead cells in the medium of cultured eukaryotic cells as marker. *J. Biotechnol.* **1992**, *25* (3), 231–243.
- Petronilli, V.; Miotto, G.; Canton, M.; Brini, M.; Colonna, R.; Bernardi, P.; Di Lisa, F. Transient and long-lasting openings of the mitochondrial permeability transition pore can be monitored directly in intact cells by changes in mitochondrial calcein fluorescence. *Biophys. J.* **1999**, *76* (2), 725–734.
- Vermes, I.; Haanen, C.; Steffens-Nakken, H.; Reutelingsperger, C. A novel assay for apoptosis. Flow cytometric detection of phosphatidylserine expression on early apoptotic cells using fluorescein labelled Annexin V. *J. Immunol. Methods* **1995**, *184* (1), 39–51.
- Chong, P. K.; Gan, C. S.; Pham, T. K.; Wright, P. C. Isobaric tags for relative and absolute quantitation (iTRAQ) reproducibility: Implication of multiple injections. *J. Proteome Res.* **2006**, *5* (5), 1232–1240.
- Seo, S. Y.; Kim, E. Y.; Kim, H.; Gwag, B. J. Neuroprotective effect of high glucose against NMDA, free radical, and oxygen-glucose deprivation through enhanced mitochondrial potentials. *J. Neurosci.* **1999**, *19* (20), 8849–8855.
- Tsujimoto, Y.; Shimizu, S. Role of the mitochondrial membrane permeability transition in cell death. *Apoptosis* **2007**, *12* (5), 835–840.
- Nakagawa, T.; Shimizu, S.; Watanabe, T.; Yamaguchi, O.; Otsu, K.; Yamagata, H.; Inohara, H.; Kubo, T.; Tsujimoto, Y. Cyclophilin D-dependent mitochondrial permeability transition regulates some necrotic but not apoptotic cell death. *Nature* **2005**, *434* (7033), 652–658.
- Jin, J.; Park, J.; Kim, K.; Kang, Y.; Park, S. G.; Kim, J. H.; Park, K. S.; Jun, H.; Kim, Y. Detection of differential proteomes of human $I\beta$ -Cells during islet-like differentiation using iTRAQ labeling. *J. Proteome Res.* **2009**, *8* (3), 1393–1403.
- Chee, S. G.; Poh, K. C.; Trong, K. P.; Wright, P. C. Technical, experimental, and biological variations in isobaric tags for relative and absolute quantitation (iTRAQ). *J. Proteome Res.* **2007**, *6* (2), 821–827.
- Glen, A.; Gan, C. S.; Hamdy, F. C.; Eaton, C. L.; Cross, S. S.; Catto, J. W. F.; Wright, P. C.; Rehman, I. iTRAQ-facilitated proteomic analysis of human prostate cancer cells identifies proteins associated with progression. *J. Proteome Res.* **2008**, *7* (3), 897–907.
- Hata, R.; Maeda, K.; Hermann, D.; Mies, G.; Hossmann, K. A. Dynamics of regional brain metabolism and gene expression after middle cerebral artery occlusion in mice. *J. Cereb. Blood Flow Metab.* **2000**, *20* (2), 306–315.
- Paschen, W.; Proud, C. G.; Mies, G. Shut-down of translation, a global neuronal stress response: Mechanisms and pathological relevance. *Curr. Pharm. Des.* **2007**, *13* (18), 1887–1902.
- Deocaris, C. C.; Kaul, S. C.; Wadhwa, R. From proliferative to neurological role of an hsp70 stress chaperone, mortalin. *Biogerontology* **2008**, *9* (6), 391–403.
- Kaufman, R. J. Stress signaling from the lumen of the endoplasmic reticulum: Coordination of gene transcriptional and translational controls. *Genes Dev.* **1999**, *13* (10), 1211–1233.
- Lo, E. H.; Dalkara, T.; Moskowitz, M. A. Mechanisms, challenges and opportunities in stroke. *Nat. Rev. Neurosci.* **2003**, *4* (5), 399–415.

- (27) Lo, E. H.; Moskowitz, M. A.; Jacobs, T. P. Exciting, radical, suicidal: How brain cells die after stroke. *Stroke* **2005**, *36* (2), 189–192.
- (28) Takagi, Y.; Tokime, T.; Nozaki, K.; Gon, Y.; Kikuchi, H.; Yodoi, J. Redox control of neuronal damage during brain ischemia after middle cerebral artery occlusion in the rat: Immunohistochemical and hybridization studies of thioredoxin. *J. Cereb. Blood Flow Metab.* **1998**, *18* (2), 206–214.
- (29) Hattori, I.; Takagi, Y.; Nozaki, K.; Kondo, N.; Bai, J.; Nakamura, H.; Hashimoto, N.; Yodoi, J. Hypoxia-ischemia induces thioredoxin expression and nitrotyrosine formation in new-born rat brain. *Redox Rep.* **2002**, *7* (5), 256–259.
- (30) Fatma, N.; Kubo, E.; Sen, M.; Agarwal, N.; Thoreson, W. B.; Camras, C. B.; Singh, D. P. Peroxiredoxin 6 delivery attenuates TNF- α - and glutamate-induced retinal ganglion cell death by limiting ROS levels and maintaining Ca²⁺ homeostasis. *Brain Res.* **2008**, *1233* (C), 63–78.
- (31) Pignataro, G.; Scorziello, A.; Di Renzo, G.; Annunziato, L. Post-ischemic brain damage: Effect of ischemic preconditioning and postconditioning and identification of potential candidates for stroke therapy. *FEBS J.* **2009**, *276* (1), 46–57.
- (32) Flower, R. J. Lipocortin. *Prog. Clin. Biol. Res.* **1990**, *349*, 11–25.
- (33) Eberhard, D. A.; Brown, M. D.; Vandenberg, S. R. Alterations of annexin expression in pathological neuronal and glial reactions: Immunohistochemical localization of annexins I, II (p36 and p11 subunits), IV, and VI in the human hippocampus. *Am. J. Pathol.* **1994**, *145* (3), 640–649.
- (34) Liu, N.; Han, S.; Lu, P. H.; Xu, X. M. Upregulation of annexins I, II, and V after traumatic spinal cord injury in adult rats. *J. Neurosci. Res.* **2004**, *77* (3), 391–401.
- (35) Nijtmans, L. G. J.; De Jong, L.; Sanz, M. A.; Coates, P. J.; Berden, J. A.; Back, J. W.; Muijsers, A. O.; Van Der Spek, H.; Grivell, L. A. Prohibitins act as a membrane-bound chaperone for the stabilization of mitochondrial proteins. *EMBO J.* **2000**, *19* (11), 2444–2451.
- (36) Liu, X.; Ren, Z.; Zhan, R.; Wang, X.; Zhang, Z.; Leng, X.; Yang, Z.; Qian, L. Prohibitin protects against oxidative stress-induced cell injury in cultured neonatal cardiomyocyte. *Cell Stress Chaperones* **2008**, *1*–9.
- (37) Suh, K. S.; Mutoh, M.; Gerdes, M.; Crutchley, J. M.; Mutoh, T.; Edwards, L. E.; Dumont, R. A.; Sodha, P.; Cheng, C.; Glick, A.; Yuspa, S. H. Antisense suppression of the chloride intracellular channel family induces apoptosis, enhances tumor necrosis factor α -induced apoptosis, and inhibits tumor growth. *Cancer Res.* **2005**, *65* (2), 562–571.
- (38) Schlattner, U.; Tokarska-Schlattner, M.; Wallimann, T. Mitochondrial creatine kinase in human health and disease. *Biochim. Biophys. Acta* **2006**, *1762* (2), 164–180.
- (39) Kowara, R.; Moraleja, K. L.; Chakravarthy, B. PLA2 signaling is involved in calpain-mediated degradation of synaptic dihydropyrimidinase-like 3 protein in response to NMDA excitotoxicity. *Neurosci. Lett.* **2008**, *430* (3), 197–202.
- (40) Schroeder, J. M.; Liu, W.; Curthoys, N. P. pH-responsive stabilization of glutamate dehydrogenase mRNA in LLC-PK₁-F⁺ cells. *Am. J. Physiol.: Renal Physiol.* **2003**, *285*, F258–265.
- (41) Zoratti, M.; Szabo, I. The mitochondrial permeability transition. *Biochim. Biophys. Acta* **1995**, *1241* (2), 139–176.
- (42) Wang, X. The expanding role of mitochondria in apoptosis. *Genes Dev.* **2001**, *15* (22), 2922–2933.
- (43) Shoshan-Barmatz, V.; Israelson, A.; Brdiczka, D.; Sheu, S. S. The voltage-dependent anion channel (VDAC): Function in intracellular signalling, cell life and cell death. *Curr. Pharm. Des.* **2006**, *12* (18), 2249–2270.
- (44) Zheng, Y.; Shi, Y.; Tian, C.; Jiang, C.; Jin, H.; Chen, J.; Almasan, A.; Tang, H.; Chen, Q. Essential role of the voltage-dependent anion channel (VDAC) in mitochondrial permeability transition pore opening and cytochrome c release induced by arsenic trioxide. *Oncogene* **2004**, *23* (6), 1239–1247.
- (45) Berman, S. B.; Watkins, S. C.; Hastings, T. G. Quantitative biochemical and ultrastructural comparison of mitochondrial permeability transition in isolated brain and liver mitochondria: Evidence for reduced sensitivity of brain mitochondria. *Exp. Neurol.* **2000**, *164* (2), 415–425.
- (46) Eliseev, R. A.; Filippov, G.; Velos, J.; VanWinkle, B.; Goldman, A.; Rosier, R. N.; Gunter, T. E. Role of cyclophilin D in the resistance of brain mitochondria to the permeability transition. *Neurobiol. Aging* **2007**, *28* (10), 1532–1542.
- (47) Schinzel, A. C.; Takeuchi, O.; Huang, Z.; Fisher, J. K.; Zhou, Z.; Rubens, J.; Hetz, C.; Danial, N. N.; Moskowitz, M. A.; Korsmeyer, S. J. Cyclophilin D is a component of mitochondrial permeability transition and mediates neuronal cell death after focal cerebral ischemia. *Proc. Natl. Acad. Sci. U.S.A.* **2005**, *102* (34), 12005–12010.
- (48) Aleyasin, H.; Rousseaux, M. W. C.; Phillips, M.; Kim, R. H.; Bland, R. J.; Callaghan, S.; Slack, R. S.; During, M. J.; Mak, T. W.; Park, D. S. The Parkinson's disease gene DJ-1 is also a key regulator of stroke-induced damage. *Proc. Natl. Acad. Sci. U.S.A.* **2007**, *104* (47), 18748–18753.
- (49) Yanagisawa, D.; Kitamura, Y.; Inden, M.; Takata, K.; Taniguchi, T.; Morikawa, S.; Morita, M.; Inubushi, T.; Tooyama, I.; Taira, T.; Iguchi-Arigo, S. M. M.; Akaike, A.; Ariga, H. DJ-1 protects against neurodegeneration caused by focal cerebral ischemia and reperfusion in rats. *J. Cereb. Blood Flow Metab.* **2008**, *28* (3), 563–578.
- (50) Sampayo-Reyes, A.; Zakharyan, R. A. Inhibition of human glutathione S-transferase omega by tocopherol succinate. *Biomed. Pharmacother.* **2006**, *60* (5), 238–244.
- (51) Kölsch, H.; Linnebank, M.; Lütjohann, D.; Jessen, F.; Wüllner, U.; Harbrecht, U.; Thelen, K. M.; Kreis, M.; Hentschel, F.; Schulz, A.; Von Bergmann, K.; Maier, W.; Heun, R. Polymorphisms in glutathione S-transferase omega-1 and AD, vascular dementia, and stroke. *Neurology* **2004**, *63* (12), 2255–2260.
- (52) Kölsch, H.; Larionov, S.; Dedeck, O.; Orantes, M.; Birkenmeier, G.; Griffin, W. S. T.; Thal, D. R. Association of the glutathione S-transferase omega-1 Ala140Asp polymorphism with cerebrovascular atherosclerosis and plaque-associated interleukin-1 α expression. *Stroke* **2007**, *38* (10), 2847–2850.
- (53) Miller, J. A.; Oldham, M. C.; Geschwind, D. H. A systems level analysis of transcriptional changes in Alzheimer's disease and normal aging. *J. Neurosci.* **2008**, *28* (6), 1410–1420.
- (54) Spiechowicz, M.; Bernstein, H. G.; Dobrowolny, H.; Leśniak, W.; Mawrin, C.; Bogerts, B.; Kuńnicki, J.; Filipiek, A. Density of Sglt1-immunopositive neurons is decreased in the cerebral cortex of Alzheimer's disease brain. *Neurochem. Int.* **2006**, *49* (5), 487–493.
- (55) Salminen, A.; Suuronen, T.; Kaarniranta, K. ROCK, PAK, and Toll of synapses in Alzheimer's disease. *Biochem. Biophys. Res. Commun.* **2008**, *371* (4), 587–590.
- (56) Lohoff, F. W.; Weller, A. E.; Bloch, P. J.; Nall, A. H.; Ferraro, T. N.; Berrettini, W. H. Association between polymorphisms in the vesicle-associated membrane protein-associated protein (VAPA) gene on chromosome 18p and bipolar disorder. *J. Neural Transm.* **2008**, *115* (9), 1339–1345.
- (57) Manabe, T.; Katayama, T.; Sato, N.; Gomi, F.; Hitomi, J.; Yanagita, T.; Kudo, T.; Honda, A.; Mori, Y.; Matsuzaki, S.; Imaizumi, K.; Mayeda, A.; Tohyama, M. Induced HMGA 1a expression causes aberrant splicing a Presenilin-2 pre-mRNA in sporadic Alzheimer's disease. *Cell Death Differ.* **2003**, *10* (6), 698–708.
- (58) Schurr, A. Energy metabolism, stress hormones and neural recovery from cerebral ischemia/hypoxia. *Neurochem. Int.* **2002**, *41* (1), 1–8.

PR900829H